Journal of Systems Engineering and Electronics
Vol. 34, No. 6, December 2023, pp.1419 – 1431

Minimum-energy leader-following formation of distributed multi-agent systems with communication constraints

QIN Donghao, WANG Le, GAO Jiuan, and XI Jianxiang*

Rocket Force University of Engineering, Xi'an 710025, China

Abstract: This paper concerns minimum-energy leader-following formation design and analysis problems of distributed multi-agent systems (DMASs) subjected to randomly switching topologies and aperiodic communication pauses. The critical feature of this paper is that the energy consumption during the formation control process is restricted by the minimum-energy constraint in the sense of the linear matrix inequality. Firstly, the leader-following formation control protocol is proposed based on the relative state information of neighboring agents, where the total energy consumption is considered. Then, minimum-energy leader-following formation design and analysis criteria are presented in the form of the linear matrix inequality, which can be checked by the generalized eigenvalue method. Especially, the value of the minimum-energy constraint is determined. An illustrative simulation is provided to show the effectiveness of the main results.

Keywords: multi-agent system, leader-following formation, communication pause, minimum energy.

DOI: 10.23919/JSEE.2023.000141

1. Introduction

Formation control of distributed multi-agent systems (DMASs) has shown an increased research interest in communities of control systems in recent years, which has a broad range of applications in various areas, such as multiple mobile robots [1,2], distributed sensor networks [3,4], unmanned aerial vehicles [5,6], and satellite groups [7−9]. Now, many approaches have been developed for formation control problems, such as virtual-structure-based strategy [10], behavior-based strategy [11,12], leader-follower-based strategy [13], and consensus-based strategy [14,15], and so on. In [16], it was proved that the former three strategies are the special cases of the consensus-based formation strategy.

The cooperative formation can carry out various complex tasks with remarkable efficiency, wide coverage, strong fault tolerance, and high-level security, which is an important research direction of DMASs. Generally, according to the topology structure of DMAS, the cooperative formation can be categorized into two cases: the leaderless formation and the leader-following formation. Different from the leaderless formation control, the leader-following formation control tries to guide the DMAS tracking a desired trajectory by using just a singular agent (or a subset of agents) that is called the leader(s), and other agents that are referred to as followers, which are driven with a time-varying (or time-invariant) geometric structure to track the leader(s). In [17], it was verified that the leader-following configuration can enhance the communication and orientation of the flock, and is also an energy saving mechanism in many biological systems. Leader-following formation problems of first-order multi-robots with a virtual leader were studied in [18], where the desired trajectory was determined by the virtual leader. Brinon-Arranz et al. [19] investigated the elastic formation tracking problems for nonlinear multi-agent systems, where all the agents can converge to a circular motion with the center tracking a time-varying reference. In [20], the leader-following networked mobile robot formation problem with unknown slippage effects for collision avoidance was investigated. Yan et al. [21] addressed the observer-based time-varying leader-following formation problem for DMASs with the one-sided Lipschitz nonlinear and quadratic inner-boundedness nonlinear dynamics, which can guarantee less conservatism and more generality with large Lipschitz constants.

The whole interactions among the DMAS play critical roles for the formation achievement. When DMASs perform complex tasks, the interaction topology may be switched as required, which leads to interaction channels

Manuscript received September 10, 2022.
*Corresponding author.
This work was supported by the National Natural Science Foundation of China (62176263;62103434;62003363), the Science Foundation for Distinguished Youth of Shaanxi Province (2021JC-35), the Youth Talent Promotion Program of Shaanxi Provincial Association for Science and Technology (20220123), the Natural Science Basic Research Program of Shaanxi Province (2022KJXX-99), and the National Defense Basic Research Program of Technology and Industry for National Defense (JCKY2021912B001).

among agents to be on or off for an indefinite time interval. All the possible interaction topologies form a switching set for the DMAS to choose. In addition, due to sensor failure, electronic interference, data packet loss etc., or to avoid enemy monitoring, there may be no any information transmission among all the agents in aperiodic time intervals, which are time stages of communication pauses. Generally speaking, it is of great significance to study communication constraints of the co-existence randomly switching topologies and aperiodic communication pauses for some specific applications. In [22], the time-varying formation control problem of singular multiagent systems with switching topologies was investigated based on the outputs of systems. Xi et al. [23] addressed the time-varying DMAS formation problems with the given energy constraint under the situation of switching topologies. In [24], a solution for the time-invariant formation control problem of a single-master-multislave bilateral teleoperator system in the presence of communication pauses was provided. Chai et al. [25] verified that the computation cost is greatly reduced for the fixed-time event-triggered time-varying formation tracking of leader-following DMASs with communication pauses than that with continuous time.

To reduce the energy consumption during the cooperative control process, a design index function of the energy consumption is usually constructed to be optimized. It is required that the index to be bounded for collaborative tasks, where the guaranteed-cost strategy is a typical one. Based on the linear quadratic regulator, Cao et al. [26] proposed two global cost functions for multivehicle systems: interaction-free and interaction-related cost functions. In [27], based on the linear matrix inequality method, guaranteed-cost consensus control criteria for general high-order DMASs with sampled-data information were given, and the corresponding guaranteed-cost values was obtained. Wang et al. [28] proposed scalable guaranteed-cost consensus design and analyzed criteria for general high-order multi-agent systems with time delays, and corresponding formulations of the upper bound of guaranteed-cost functions were derived. In [29], robust H_∞ guaranteed-cost time-varying DMAS formation problems with time-varying delays and external disturbances were investigated, and sufficient conditions with H_∞ disturbance attenuation performance were derived. However, the bounds derived in [26−29] may not be minimal. In general, it is a way to minimize energy consumption by designing reasonable energy constraints to restrict the upper bound value of guaranteed cost. Combining with above introductions of the formation, communication constraints, and guaranteed-cost strategy of DMASs, to the best of our knowledge, there are few literatures reported on the study of the minimum-energy leader-following formation with communication constraints of randomly switching topologies and aperiodic communication pauses.

In this paper, minimum-energy leader-following formation control problems for DMASs are investigated, which are subjected to communication constraints of randomly switching topologies and aperiodic communication pauses. By considering the local information from neighboring agents of the whole system, a distributed control protocol is proposed with the total energy consumption of all the agents being involved. With the state space decomposition method, the closed-loop system is divided into two subsystems, which correspond to the macroscopically whole motion of the DMAS and the microcosmically relative motion of followers, where the macroscopically whole motion can be regarded to be dictated by the leader. To minimize the total energy consumption during the formation process, minimum-energy criteria are presented to restrict the total energy consumption of the whole DMAS. By the criteria, it can not only guarantee the formation achievement but also ensure the energy consumption during the formation control process to be minimal in the sense of the linear matrix inequality.

The novelties and primary contributions of this paper are listed as follows. (i) Problems of minimum-energy consumption for leader-following formation are studied，while the guaranteed-cost strategy proposed in [26−29] cannot ensure the total energy consumption during the cooperative control to be minimal. By the constructed constraint for restricting the energy consumption to be minimal, an additional linear matrix is derived as an important term of minimum-energy formation criteria. The criteria can be checked by the generalized eigenvalue method. (ii) Communication constraints of the co-existence of randomly switching topology and aperiodic communication pauses are dealt with, while DMAS formation problems in the case of either switching topologies or communication pauses are studied in [22−25,30]. In this study, the whole time is modeled as time intervals by time intervals, where each interval contains two subintervals, and the convergent quantity of the constructed Lyapunov function candidate in the switching topology subinterval is required to be greater than the divergent quantity in the communication pause subinterval in each interval. Thus, the global convergence can be ensured and the leader-follow formation is achievable.

The rest arrangement of this paper is structured as follows. Section 2 introduces some preliminaries and the problem description. Design and analysis criteria of the minimum-energy leader-following formation are proposed in Section 3. In Section 4, a numerical example is given to show the effectiveness of the theoretical results. Section 5 summarizes the whole work of this paper.

Throughout this paper, the following notations are the main symbols applied. $\mathbf{N}$ denotes the set of nonnegative integer numbers, $\mathbf{R}$, $\mathbf{R}^d$, and $\mathbf{R}^{d\times m}$ denote sets of real numbers, d-dimensional real column vectors and $d\times m$-dimensional real matrices, respectively. $\mathbf{1}_N$ denotes an $N\times 1$ column vector of all elements being 1, and $\boldsymbol{I}_N$ denotes an N-dimensional identity matrix. 0 is zero number, and $\mathbf{0}$ denotes zero vector or zero matrix respectively. $\hat{\boldsymbol{Q}}>0$ or $\hat{\boldsymbol{Q}}<0$ denotes that $\hat{\boldsymbol{Q}}$ is positive or negative definite matrix, and $\hat{\boldsymbol{Q}}^{\mathrm{T}}$ denotes the transpose of matrix $\hat{\boldsymbol{Q}}$. $\hat{\boldsymbol{Q}}^{\mathrm{T}}=\hat{\boldsymbol{Q}}$ denotes that $\hat{\boldsymbol{Q}}$ is a symmetric matrix, $\times$ denotes Kronecker product.

2. Preliminaries and problem description

2.1 Graph theory

For a DMAS with n agents, the interacted information flow among agents is incorporated into a topology graph $\mathcal{G}=(\mathcal{V},\mathcal{E},\mathcal{W})$, where $\mathcal{V}=\{v_i|i=1,2,\cdots,n\}$ is the node set with v_i denoting agent i, $\mathcal{E}\subseteq\{(v_i,v_k):v_i,v_k\in\mathcal{V}\}$ (i, $k=1,2,\cdots,n$) is the edge set with (v_i,v_k) representing the communication channel from agent k to agent i, and $\mathcal{W}=[w_{ik}]\in\mathbf{R}^{n\times n}$ indicates a weighted adjacency matrix with $w_{ik}\geqslant 0$ denoting the interaction weight. If and only if there is a connected channel between v_i and v_k, then $w_{ik}>0$; otherwise, $w_{ik}=0$ ($i\neq k$). Each agent is assumed to contain no self-loop; that is, $w_{ii}=0$ ($i\in\{1,2,\cdots,n\}$). $\mathcal{N}_i=\{v_k\in\mathcal{V}|(v_k,v_i)\in\mathcal{E}\}$ represents the neighboring set of v_i. The Laplacian matrix $\boldsymbol{L}=\mathcal{D}-\mathcal{W}$ is utilized to describe the algebraic feature of the topology graph, where $\mathcal{D}=\mathrm{diag}\{d_1,d_2,\cdots,d_n\}$ with $d_i=\sum_{k=1}^{n}w_{ik}$ ($i=1,2,\cdots,n$) being the in-degree diagonal matrix of the graph. A directed path between two nonneighboring agents v_i and v_j is a finite ordered sequence of distinct edges with the form $(v_i,v_{\theta 1})$, $(v_{\theta 1},v_{\theta 2})$,$\cdots$, $(v_{\theta q},v_j)$. In the topology graph, if there is a directed path from v_i to every other node, then a spanning tree exists and v_i is called the root node. More details can refer to [31].

2.2 Communication constraints

To facilitate research, a mathematical model for communication constraints of randomly switching topologies and aperiodic communication pauses is described as follows. Let $[t_p,t_{p+1})$ ($p\in\mathbf{N}$) denote an infinite sequence of nonoverlapping time intervals, and the maximum time interval and the minimum time interval are $t_{\max}=\max\{t_{p+1}-t_p:p\in\mathbf{N}\}$ and $t_{\min}=\min\{t_{p+1}-t_p:p\in\mathbf{N}\}$, respectively. Each interval $[t_p,t_{p+1})$ ($p\in\mathbf{N}$) contains a switching topology subinterval $[t_p,\tilde{t}_p)$ and a communication pause subinterval $[\tilde{t}_p,t_{p+1})$. The corresponding communication pause rate is $\omega_p=(t_{p+1}-\tilde{t}_p)/(t_{p+1}-t_p)$, and $\hat{\omega}$ is set as the maximum communication pause rate of all the time intervals; that is, $0\leqslant\omega_p\leqslant\hat{\omega}<1$ ($p\in\mathbf{N}$). In the switching topology subinterval $[t_p,\tilde{t}_p)$ ($p\in\mathbf{N}$), the index set of the switching topology is represented by $\chi\in\{l|l=1,2,\cdots,s\}$, and the switching signal is $\sigma(t):[0,+\infty)\to\chi$, which implies that the topologies switch in accordance with the signal $\sigma(t)$. In the communication pause subinterval $[\tilde{t}_p,t_{p+1})$ ($p\in\mathbf{N}$), there are not any interconnected channels among all the agents, which means that the Laplacian matrix $\boldsymbol{L}=\mathbf{0}$.

This paper investigates the leader-following DMAS formation problem with randomly switching topologies and aperiodic communication pauses. In the leader-following DMAS, the interconnected channels among followers are bidirectional with the same weight, but they are unidirectional from the leader to followers, which imply that the leader can send information to followers but does not receive information from followers. Therefore, the Laplacian matrix of the topology of the leader-following DMAS is asymmetric. Moreover, it is assumed that there is at least one spanning tree in each topology graph of the switching set, where the leader is assigned as the root node in the topology graph.

2.3 Problem description

Consider a leader-following DMAS with N agents, where agent 1 is assigned as the leader and agent i ($i=2,3,\cdots,N$) are followers. The dynamics of leader and agent i ($i=2,3,\cdots,N$) are described as

$$\begin{cases}\dot{\boldsymbol{x}}_1(t)=\boldsymbol{A}\boldsymbol{x}_1(t)\\ \dot{\boldsymbol{x}}_i(t)=\boldsymbol{A}\boldsymbol{x}_i(t)+\boldsymbol{B}\boldsymbol{u}_i(t)\end{cases}\tag{1}$$

where $\boldsymbol{A}\in\mathbf{R}^{d\times d}$ is the system matrix, $\boldsymbol{B}\in\mathbf{R}^{d\times m}$ is the control input matrix, $\boldsymbol{u}_i(t)\in\mathbf{R}^m$ is the control input variable of agent i, and $\boldsymbol{x}_1(t)\in\mathbf{R}^d$ and $\boldsymbol{x}_i(t)\in\mathbf{R}^d$ are the state variables of leader and agent i, respectively.

Let the time-varying function $\boldsymbol{f}(t)=[\boldsymbol{f}_1^{\mathrm{T}}(t),\boldsymbol{f}_2^{\mathrm{T}}(t),\cdots,\boldsymbol{f}_N^{\mathrm{T}}(t)]^{\mathrm{T}}$ with $\boldsymbol{f}_1(t)\equiv\mathbf{0}$ represent the desired time-varying formation of the leader-following DMAS, then the formation control protocol in the interval $[t_p,t_{p+1})$ is proposed as follows:

$$\begin{cases}\boldsymbol{u}_i(t)=\boldsymbol{u}_{i1}(t)+\boldsymbol{u}_{ik}(t),\ \ t\in[t_p,\tilde{t}_p)\\ \boldsymbol{u}_{i1}(t)=w_{\sigma(t)}^{i1}\boldsymbol{K}(\boldsymbol{x}_1(t)-\boldsymbol{x}_i(t)+\boldsymbol{f}_i(t))\\ \boldsymbol{u}_{ik}(t)=\boldsymbol{K}\sum\limits_{k\in\mathcal{N}_{\sigma(t)}^i}w_{\sigma(t)}^{ik}(\boldsymbol{x}_k(t)-\boldsymbol{x}_i(t)-\boldsymbol{f}_k(t)+\boldsymbol{f}_i(t))\\ \boldsymbol{u}_i(t)=\mathbf{0},\ \ t\in[\tilde{t}_p,t_{p+1})\\ E=\sum\limits_{i=2}^{N}\int_0^{+\infty}\boldsymbol{u}_i^{\mathrm{T}}(t)\hat{\boldsymbol{Q}}\boldsymbol{u}_i(t)\mathrm{d}t\end{cases}\tag{2}$$

where $i=2,3,\cdots,N$, $p\in\mathbf{N}$, $\boldsymbol{f}_i(t)\in\mathbf{R}^d$ is a piecewise con-

tinuous differentiable formation function, $\boldsymbol{K}\in\mathbf{R}^{m\times d}$ is the gain matrix, $w_{\sigma(t)}^{ik}$ and $u_{ik}(t)$ $(k=1,2,\cdots,N)$ are the interaction weight and the control input from the agent k to agent i, respectively, $\hat{\boldsymbol{Q}}\in\mathbf{R}^{m\times m}$ with $\hat{\boldsymbol{Q}}=\hat{\boldsymbol{Q}}^{\mathrm{T}}>0$ is the weighted matrix, and $\mathcal{N}_{\sigma(t)}^{i}$ is the neighboring set of follower i. The symbol $E>0$ represents the total energy consumption of the leader-following DMAS. The definition of the leader-following DMAS formation achievable with the total energy consumption E being minimum.

Definition 1 For any bounded disagreement initial conditions $\boldsymbol{x}_i(0)-\boldsymbol{f}_i(0)$ $(i=1,2,\cdots,N)$, DMAS (1) with control protocol (2) is said to be minimum-energy leader-following formation achievable if there exists a gain matrix $\boldsymbol{K}$ such that $\lim\limits_{t\to+\infty}(\boldsymbol{x}_i(t)-\boldsymbol{f}_i(t)-\boldsymbol{x}_1(t))=\boldsymbol{0}$ and $E\leqslant E_{\min}$, where $E_{\min}$ is the minimum-energy constraint.

The main objective of this paper focuses on two problems as follows: (i) Determine the gain matrix $\boldsymbol{K}$ such that leader-following DMAS (1) with control protocol (2) can achieve the minimum-energy time-varying formation. (ii) Propose sufficient conditions of the minimum-energy leader-following formation achievement when the gain matrix $\boldsymbol{K}$ is given in advance. Main difficulties lie in how to determine the minimum-energy constraint of the leader-following DMAS with communication constraints of randomly switching topologies and aperiodic communication pauses.

Remark 1 Less energy consumption is of great significance in practical engineer applications. The guaranteed-cost strategy aims to determine the upper bound of performance index, but it cannot ensure the energy consumption during the formation control process to be minimum, while the minimum-energy formation strategy is proposed to minimize the energy consumption by designing some optimization procedure. The formation control protocol (2) gives the formula of the total energy consumption, which is the sum of the quadratic integral function of energy consumptions of all followers. Thus, the relationship between the total energy consumption E and the control gain matrix $\boldsymbol{K}$ is established. In addition, the control input of each agent is analyzed by interval, where each interval is divided into two subintervals; that is, the switching topology subinterval and the communication pause subinterval. In the switching topology subinterval, the control input of each follower comes from neighboring followers and the leader. In the communication pauses, no control input exists because there is no interaction channel among all the agents.

3. Minimum-energy leader-following formation design and analysis criteria

In this section, minimum-energy leader-following formation problems of the DMAS are studied, which is subjected to randomly switching topologies and aperiodic communication pauses. Firstly, the formation achievable problem is transformed into an asymptotic stability problem. Then, leader-following formation design criteria with the minimum-energy constraint are proposed in terms of the linear matrix inequality tool, which can be checked by the generalized eigenvalue approach.

Let $\bar{\boldsymbol{x}}_i(t)=\boldsymbol{x}_i(t)-\boldsymbol{f}_i(t)$ $(i\in\{1,2,\cdots,N\})$ be the formation tracking error vector function of agent i, then the compact form of the whole dynamics of leader-following DMAS (1) with control protocol (2) can be written as follows:

$$\begin{cases}\dot{\bar{\boldsymbol{x}}}(t)=(\boldsymbol{I}_N\otimes\boldsymbol{A})(\bar{\boldsymbol{x}}(t)-\boldsymbol{f}(t))-\\ \qquad(\boldsymbol{L}_{\sigma(t)}\otimes\boldsymbol{BK})\bar{\boldsymbol{x}}(t)-\dot{\boldsymbol{f}}(t),\ t\in[t_p,\tilde{t}_p)\\ \dot{\bar{\boldsymbol{x}}}(t)=(\boldsymbol{I}_N\otimes\boldsymbol{A})(\bar{\boldsymbol{x}}(t)-\boldsymbol{f}(t))-\dot{\boldsymbol{f}}(t),\ t\in[\tilde{t}_p,t_{p+1})\end{cases}\tag{3}$$

where $p\in\mathbf{N}$, $\boldsymbol{f}(t)=[\boldsymbol{f}_1^{\mathrm{T}}(t),\boldsymbol{f}_2^{\mathrm{T}}(t),\cdots,\boldsymbol{f}_N^{\mathrm{T}}(t)]^{\mathrm{T}}$ with $\boldsymbol{f}_1(t)\equiv\boldsymbol{0}$, $\bar{\boldsymbol{x}}(t)=[\boldsymbol{x}_1^{\mathrm{T}}(t),\bar{\boldsymbol{x}}_2^{\mathrm{T}}(t),\cdots,\bar{\boldsymbol{x}}_N^{\mathrm{T}}(t)]^{\mathrm{T}}$, and $\boldsymbol{L}_{\sigma(t)}$ is the Laplacian matrix of the switching topology. If $\dot{\boldsymbol{f}}_i(t)=\boldsymbol{A}\boldsymbol{f}_i(t)$ $(i=2,3,\cdots,N)$, then it can be derived that

$$\dot{\boldsymbol{f}}(t)=(\boldsymbol{I}_N\otimes\boldsymbol{A})\boldsymbol{f}(t).\tag{4}$$

Substituting (4) into (3) results in the following closed-loop system:

$$\begin{cases}\dot{\bar{\boldsymbol{x}}}(t)=(\boldsymbol{I}_N\otimes\boldsymbol{A}-\boldsymbol{L}_{\sigma(t)}\otimes\boldsymbol{BK})\bar{\boldsymbol{x}}(t),\ t\in[t_p,\tilde{t}_p)\\ \dot{\bar{\boldsymbol{x}}}(t)=(\boldsymbol{I}_N\otimes\boldsymbol{A})\bar{\boldsymbol{x}}(t),\ t\in[\tilde{t}_p,t_{p+1})\end{cases}.\tag{5}$$

Let $\boldsymbol{L}_{\sigma(t)}^{\mathrm{fl}}=\mathrm{diag}\{w_{\sigma(t)}^{21},w_{\sigma(t)}^{31},\cdots,w_{\sigma(t)}^{N1}\}$ and $\boldsymbol{l}_{\sigma(t)}^{\mathrm{fl}}=[w_{\sigma(t)}^{21},w_{\sigma(t)}^{31},\cdots,w_{\sigma(t)}^{N1}]^{\mathrm{T}}$, then the Laplacian matrix $\boldsymbol{L}_{\sigma(t)}$ of the leader-following DMAS topology in the switching subinterval $[t_p,\tilde{t}_p)$ $(p\in\mathbf{N})$ can be depicted as follows:

$$\boldsymbol{L}_{\sigma(t)}=\begin{bmatrix}0 & \boldsymbol{0}\\ -\boldsymbol{l}_{\sigma(t)}^{\mathrm{fl}} & \boldsymbol{L}_{\sigma(t)}^{\mathrm{ff}}+\boldsymbol{L}_{\sigma(t)}^{\mathrm{fl}}\end{bmatrix}\tag{6}$$

where $\boldsymbol{L}_{\sigma(t)}^{\mathrm{ff}}\in\mathbf{R}^{(N-1)\times(N-1)}$ is the Laplacian matrix of followers without considering interactions from the leader. Note that the Laplacian matrix $\boldsymbol{L}_{\sigma(t)}^{\mathrm{ff}}$ is symmetric because channels between any two interconnected followers are bidirectional with the same weight. To well deal with the impact of the asymmetry of the Laplacian matrix $\boldsymbol{L}_{\sigma(t)}$, a nonsingular matrix $\boldsymbol{U}=\begin{bmatrix}1 & \boldsymbol{0}\\ \boldsymbol{1}_{N-1} & \boldsymbol{I}_{N-1}\end{bmatrix}$ with $\boldsymbol{U}^{-1}=\begin{bmatrix}1 & \boldsymbol{0}\\ -\boldsymbol{1}_{N-1} & \boldsymbol{I}_{N-1}\end{bmatrix}$ is introduced. Due to $\boldsymbol{l}_{\sigma(t)}^{\mathrm{fl}}=\boldsymbol{L}_{\sigma(t)}^{\mathrm{fl}}\boldsymbol{1}_{N-1}$, it can be shown that

$$\hat{\boldsymbol{L}}_{\sigma(t)}=\boldsymbol{U}^{-1}\boldsymbol{L}_{\sigma(t)}\boldsymbol{U}=\begin{bmatrix}0 & \\ & \boldsymbol{L}_{\sigma(t)}^{\mathrm{ff}}+\boldsymbol{L}_{\sigma(t)}^{\mathrm{fl}}\end{bmatrix}\tag{7}$$

which has the same eigenvalues as the similar matrix $\boldsymbol{L}_{\sigma(t)}$. Because the matrix $\hat{\boldsymbol{L}}_{\sigma(t)}$ is symmetric and positive definite, there is at least one zero eigenvalue, then the

eigenvalues of the Laplacian matrix $\boldsymbol{L}_{\sigma(t)}$ can be depicted by $0=\lambda_{\sigma(t),1}\leqslant\lambda_{\sigma(t),2}\leqslant\lambda_{\sigma(t),3}\leqslant\cdots\leqslant\lambda_{\sigma(t),N}$. Furthermore, it can be found that there exists an orthogonal matrix $\bar{\boldsymbol{U}}_{\sigma(t)}^{-1}=\bar{\boldsymbol{U}}_{\sigma(t)}^{\mathrm{T}}$ such that

$$\bar{\boldsymbol{U}}_{\sigma(t)}^{\mathrm{T}}\left(\boldsymbol{L}_{\sigma(t)}^{\mathrm{ff}}+\boldsymbol{L}_{\sigma(t)}^{\mathrm{fl}}\right)\bar{\boldsymbol{U}}_{\sigma(t)}=\ \mathrm{diag}\{\lambda_{\sigma(t),2},\lambda_{\sigma(t),3},\cdots,\lambda_{\sigma(t),N}\}. \tag{8}$$

In the switching set, the minimum nonzero and maximum eigenvalues of the Laplacian matrix $\boldsymbol{L}_{\sigma(t)}$ are $\lambda_{\min}=\min\{\lambda_{\sigma(t),2},\sigma(t)\in\chi\}$ and $\lambda_{\max}=\max\{\lambda_{\sigma(t),N},\sigma(t)\in\chi\}$, respectively. Let

$$\begin{aligned}\widehat{\boldsymbol{x}}(t)=\left(\boldsymbol{U}^{-1}\otimes I_d\right)\left[\boldsymbol{x}_1^{\mathrm{T}}(t),\bar{\boldsymbol{x}}_2^{\mathrm{T}}(t),\cdots,\bar{\boldsymbol{x}}_N^{\mathrm{T}}(t)\right]^{\mathrm{T}}=\\ \left[\boldsymbol{x}_1^{\mathrm{T}}(t),\bar{\boldsymbol{x}}_2^{\mathrm{T}}(t)-\boldsymbol{x}_1^{\mathrm{T}}(t),\cdots,\bar{\boldsymbol{x}}_N^{\mathrm{T}}(t)-\boldsymbol{x}_1^{\mathrm{T}}(t)\right]^{\mathrm{T}}\end{aligned} \tag{9}$$

where $\widehat{\boldsymbol{x}}(t)=\left[\boldsymbol{x}_1^{\mathrm{T}}(t),\widehat{\boldsymbol{x}}_2^{\mathrm{T}}(t),\cdots,\widehat{\boldsymbol{x}}_N^{\mathrm{T}}(t)\right]^{\mathrm{T}}$ and $\widehat{\boldsymbol{x}}_i(t)=\bar{\boldsymbol{x}}_i(t)-\boldsymbol{x}_1(t)$ $(i=2,3,\cdots,N)$. Let

$$\hat{\boldsymbol{U}}_{\sigma(t)}^{\mathrm{T}}=\begin{bmatrix}1&\\&\bar{\boldsymbol{U}}_{\sigma(t)}^{\mathrm{T}}\end{bmatrix} \tag{10}$$

and

$$\begin{aligned}\left[\hat{\boldsymbol{x}}_2^{\mathrm{T}}(t),\hat{\boldsymbol{x}}_3^{\mathrm{T}}(t),\cdots,\hat{\boldsymbol{x}}_N^{\mathrm{T}}(t)\right]^{\mathrm{T}}=\\ \left(\overline{\boldsymbol{U}}_{\sigma(t)}^{\mathrm{T}}\otimes\boldsymbol{I}_d\right)\left[\widehat{\boldsymbol{x}}_2^{\mathrm{T}}(t),\widehat{\boldsymbol{x}}_3^{\mathrm{T}}(t),\cdots,\widehat{\boldsymbol{x}}_N^{\mathrm{T}}(t)\right]^{\mathrm{T}},\end{aligned} \tag{11}$$

then it can be deduced by (9) that

$$\begin{aligned}\left[\boldsymbol{x}_1^{\mathrm{T}}(t),\hat{\boldsymbol{x}}_2^{\mathrm{T}}(t),\hat{\boldsymbol{x}}_3^{\mathrm{T}}(t),\cdots,\hat{\boldsymbol{x}}_N^{\mathrm{T}}(t)\right]^{\mathrm{T}}=\\ \left(\hat{\boldsymbol{U}}_{\sigma(t)}^{\mathrm{T}}\otimes\boldsymbol{I}_d\right)\left[\boldsymbol{x}_1^{\mathrm{T}}(t),\widehat{\boldsymbol{x}}_2^{\mathrm{T}}(t),\widehat{\boldsymbol{x}}_3^{\mathrm{T}}(t),\cdots,\widehat{\boldsymbol{x}}_N^{\mathrm{T}}(t)\right]^{\mathrm{T}}=\\ \left(\hat{\boldsymbol{U}}_{\sigma(t)}^{\mathrm{T}}\boldsymbol{U}^{-1}\otimes\boldsymbol{I}_d\right)\left[\boldsymbol{x}_1^{\mathrm{T}}(t),\bar{\boldsymbol{x}}_2^{\mathrm{T}}(t),\cdots,\bar{\boldsymbol{x}}_N^{\mathrm{T}}(t)\right]^{\mathrm{T}}.\end{aligned} \tag{12}$$

Substituting (12) into (5), it can be found that the whole DMAS can be described by subsystems as follows:

$$\dot{\boldsymbol{x}}_1(t)=\boldsymbol{A}\boldsymbol{x}_1(t),\ t\in[t_p,t_{p+1}), \tag{13}$$

$$\begin{cases}\dot{\hat{\boldsymbol{x}}}_i(t)=(\boldsymbol{A}-\lambda_{\sigma(t),i}\boldsymbol{B}\boldsymbol{K})\hat{\boldsymbol{x}}_i(t),\ t\in[t_p,\tilde{t}_p)\\ \dot{\hat{\boldsymbol{x}}}_i(t)=\boldsymbol{A}\hat{\boldsymbol{x}}_i(t),\ t\in[\tilde{t}_p,t_{p+1})\end{cases}, \tag{14}$$

where $i=2,3,\cdots,N$ and $p\in\mathbf{N}$.

Define

$$\boldsymbol{V}_z(t)\triangleq\left(\boldsymbol{U}\hat{\boldsymbol{U}}_{\sigma(t)}\otimes\boldsymbol{I}_d\right)\left[\boldsymbol{x}_1^{\mathrm{T}}(t),\boldsymbol{0},\cdots,\boldsymbol{0}\right]^{\mathrm{T}}, \tag{15}$$

$$\boldsymbol{V}_{\bar{z}}(t)\triangleq\left(\boldsymbol{U}\hat{\boldsymbol{U}}_{\sigma(t)}\otimes\boldsymbol{I}_d\right)\left[\boldsymbol{0},\hat{\boldsymbol{x}}_2^{\mathrm{T}}(t),\cdots,\hat{\boldsymbol{x}}_N^{\mathrm{T}}(t)\right]^{\mathrm{T}}, \tag{16}$$

where $\boldsymbol{U}\hat{\boldsymbol{U}}_{\sigma(t)}$ is the decomposition matrix, it can be shown by (12) that

$$\bar{\boldsymbol{x}}(t)=\boldsymbol{V}_z(t)+\boldsymbol{V}_{\bar{z}}(t) \tag{17}$$

which means that the closed-loop system is decomposed into two subsystems that are determined by $\boldsymbol{V}_z(t)$ and $\boldsymbol{V}_{\bar{z}}(t)$, respectively. Since $\boldsymbol{U}\hat{\boldsymbol{U}}_{\sigma(t)}$ is nonsingular, it can be found from (15)−(17) that $\boldsymbol{V}_z(t)$ and $\boldsymbol{V}_{\bar{z}}(t)$ are linearly independent, which means that closed-loop system (5) can be decomposed into two subsystems. Due to $\boldsymbol{U}\hat{\boldsymbol{U}}_{\sigma(t)}\boldsymbol{e}_1=\boldsymbol{1}_N$, it can be shown from (15) that

$$\boldsymbol{V}_z(t)=\left(\boldsymbol{U}\hat{\boldsymbol{U}}_{\sigma(t)}\right)\boldsymbol{e}_1\otimes\boldsymbol{x}_1(t)=\boldsymbol{1}_N\otimes\boldsymbol{x}_1(t). \tag{18}$$

By (16), it can be found that

$$\boldsymbol{V}_{\bar{z}}(t)=\sum_{i=2}^{N}\left(\boldsymbol{U}\hat{\boldsymbol{U}}_{\sigma(t)}\right)\boldsymbol{e}_i\otimes\hat{\boldsymbol{x}}_i(t) \tag{19}$$

where $\boldsymbol{e}_i$ is the N-dimensional column vector with the ith element being 1 and the other elements 0. By the structures of $\boldsymbol{V}_z(t)$, it can be ensured that

$$\lim_{t\to+\infty}(\bar{\boldsymbol{x}}_i(t)-\boldsymbol{x}_1(t))=\boldsymbol{0}, \tag{20}$$

if and only if $\lim\limits_{t\to+\infty}\hat{\boldsymbol{x}}_i(t)=\boldsymbol{0}$ $(i=2,3,\cdots,N)$. In this scenario, due to $\bar{\boldsymbol{x}}_i(t)=\boldsymbol{x}_i(t)-\boldsymbol{f}_i(t)$, it can be obtained that

$$\lim_{t\to+\infty}(\boldsymbol{x}_i(t)-\boldsymbol{f}_i(t)-\boldsymbol{x}_1(t))=\boldsymbol{0}. \tag{21}$$

Thus, it means that the leader-following DMAS is formation achievable according to Definition 1. From the above analysis, it can be found that the macroscopically whole motion of all the followers is determined by subsystem (13); that is, the dynamics of the leader. The microcosmically relative motion of followers is depicted by subsystem (14). Based on the aforementioned derivation, it can be found that leader-following DMAS (1) with control protocol (2) is formation achievable if and only if subsystem (14) is asymptotically stable, which implies that the leader-following formation control problem is converted into an asymptotic stability problem.

Remark 2 The Laplacian matrix of the topology graph of the leader-following DMAS is asymmetric, which leads to some difficulties in the design and analysis of the formation problem with minimum-energy constraint. In this case, a constant nonsingular matrix $\boldsymbol{U}=\begin{bmatrix}1&\boldsymbol{0}\\ \boldsymbol{1}_{N-1}&\boldsymbol{I}_{N-1}\end{bmatrix}$ with the special structure is introduced, which is used to transform the asymmetric Laplacian matrix $\boldsymbol{L}_{\sigma(t)}$ of the leader-following topology into a symmetric matrix $\begin{bmatrix}0&\\&\boldsymbol{L}_{\sigma(t)}^{\mathrm{ff}}+\boldsymbol{L}_{\sigma(t)}^{\mathrm{fl}}\end{bmatrix}$. Then, the time-varying matrix $\hat{\boldsymbol{U}}_{\sigma(t)}^{\mathrm{T}}=\begin{bmatrix}1&\\&\overline{\boldsymbol{U}}_{\sigma(t)}^{\mathrm{T}}\end{bmatrix}$ is established, where $\overline{\boldsymbol{U}}_{\sigma(t)}^{\mathrm{T}}$ is the orthogonal matrix that can transform the matrix $\boldsymbol{L}_{\sigma(t)}^{\mathrm{ff}}+\boldsymbol{L}_{\sigma(t)}^{\mathrm{fl}}$ into the diagonal matrix. Based on the above two-step transformation, the close-loop system can be decomposed into two subsystems to analyze the achievablity of the desired leader-following formation.

In the following, minimum-energy leader-following

formation design criteria of DMAS (1) with control protocol (2) is proposed in terms of the linear matrix inequality tool.

Theorem 1 DMAS (1) with control protocol (2) is minimum-energy leader-following formation achievable if $\dot{\boldsymbol{f}}_i(t)=\boldsymbol{A}\boldsymbol{f}_i(t)$ $(i=2,3,\cdots,N)$, $\alpha(1-\hat{\omega})>\beta\hat{\omega}\mathrm{e}^{\beta\hat{\omega}t_{\max}}$ with $\alpha>0$ and $\beta>0$, then there exists $\hat{\boldsymbol{H}}^{\mathrm{T}}=\hat{\boldsymbol{H}}>0$ such that the following minimization problem has a minimum-energy optimal parameter ℓ:

$$\min \ell$$

$$\text{s.t.}\begin{cases}\hat{\Re}_1=\boldsymbol{A}\hat{\boldsymbol{H}}+\hat{\boldsymbol{H}}\boldsymbol{A}^{\mathrm{T}}-\beta\hat{\boldsymbol{H}}<0\\ \hat{\Re}_2=\begin{bmatrix}\wp & \lambda_{\min}^{-1}\lambda_{\max}\boldsymbol{B}\hat{\boldsymbol{Q}}\\ * & -\hat{\boldsymbol{Q}}\end{bmatrix}<0\\ \hat{\Re}_3=\boldsymbol{I}_d-\ell\hat{\boldsymbol{H}}<0\end{cases}$$

where $\wp=\boldsymbol{A}\hat{\boldsymbol{H}}+\hat{\boldsymbol{H}}\boldsymbol{A}^{\mathrm{T}}-2\boldsymbol{B}\boldsymbol{B}^{\mathrm{T}}+\alpha\hat{\boldsymbol{H}}$, $*$ denotes the symmetric term of the symmetric matrix. In this case, $\boldsymbol{K}=\lambda_{\min}^{-1}\boldsymbol{B}^{\mathrm{T}}\hat{\boldsymbol{H}}^{-1}$ and the minimum-energy constraint

$$E_{\min}=\bar{\boldsymbol{x}}^{\mathrm{T}}(0)\left(\begin{bmatrix}N-1 & -\boldsymbol{1}_{N-1}^{\mathrm{T}}\\ -\boldsymbol{1}_{N-1} & \boldsymbol{I}_{N-1}\end{bmatrix}\otimes\ell\boldsymbol{I}_d\right)\bar{\boldsymbol{x}}(0).$$

Proof Take common Lyapunov function candidates for subsystems (14) as

$$V_i(t)=\hat{\boldsymbol{x}}_i^{\mathrm{T}}(t)\hat{\boldsymbol{H}}^{-1}\hat{\boldsymbol{x}}_i(t),\ \ i=2,3,\cdots,N \tag{22}$$

where $\hat{\boldsymbol{H}}^{\mathrm{T}}=\hat{\boldsymbol{H}}>0$. In the switching topology subinterval $[t_p,\tilde{t}_p)$ $(p\in\mathbf{N})$, taking the derivative of $V_i(t)$ with respect to t, by (14) and (22) it can be obtained that

$$\dot{V}_i(t)=\hat{\boldsymbol{x}}_i^{\mathrm{T}}(t)\left(\boldsymbol{A}^{\mathrm{T}}\hat{\boldsymbol{H}}^{-1}+\hat{\boldsymbol{H}}^{-1}\boldsymbol{A}\right)\hat{\boldsymbol{x}}_i(t)-$$
$$\hat{\boldsymbol{x}}_i^{\mathrm{T}}(t)\left(\lambda_{\sigma(t),i}\boldsymbol{K}^{\mathrm{T}}\boldsymbol{B}^{\mathrm{T}}\hat{\boldsymbol{H}}^{-1}+\lambda_{\sigma(t),i}\hat{\boldsymbol{H}}^{-1}\boldsymbol{B}\boldsymbol{K}\right)\hat{\boldsymbol{x}}_i(t). \tag{23}$$

Let the gain matrix $\boldsymbol{K}=\lambda_{\min}^{-1}\boldsymbol{B}^{\mathrm{T}}\hat{\boldsymbol{H}}^{-1}$, then it immediately follows from (23) that

$$\dot{V}_i(t)=\hat{\boldsymbol{x}}_i^{\mathrm{T}}(t)\hat{\boldsymbol{H}}^{-1}\left(\boldsymbol{A}\hat{\boldsymbol{H}}+\hat{\boldsymbol{H}}\boldsymbol{A}^{\mathrm{T}}\right)\hat{\boldsymbol{H}}^{-1}\hat{\boldsymbol{x}}_i(t)-$$
$$2\lambda_{\sigma(t),i}\lambda_{\min}^{-1}\hat{\boldsymbol{x}}_i^{\mathrm{T}}(t)\hat{\boldsymbol{H}}^{-1}\boldsymbol{B}\boldsymbol{B}^{\mathrm{T}}\hat{\boldsymbol{H}}^{-1}\hat{\boldsymbol{x}}_i(t). \tag{24}$$

Due to $\lambda_{\sigma(t),i}\lambda_{\min}^{-1}\geqslant 1$, it can be found by (24) that

$$\dot{V}_i(t)\leqslant\hat{\boldsymbol{x}}_i^{\mathrm{T}}(t)\hat{\boldsymbol{H}}^{-1}\left(\boldsymbol{A}\hat{\boldsymbol{H}}+\hat{\boldsymbol{H}}\boldsymbol{A}^{\mathrm{T}}-2\boldsymbol{B}\boldsymbol{B}^{\mathrm{T}}\right)\hat{\boldsymbol{H}}^{-1}\hat{\boldsymbol{x}}_i(t). \tag{25}$$

Let

$$\hat{\boldsymbol{M}}_1=\boldsymbol{A}\hat{\boldsymbol{H}}+\hat{\boldsymbol{H}}\boldsymbol{A}^{\mathrm{T}}-2\boldsymbol{B}\boldsymbol{B}^{\mathrm{T}}+\alpha\hat{\boldsymbol{H}}<0,\ \ \alpha>0, \tag{26}$$

then it can be proved by (22) and (25) that

$$\dot{V}_i(t)<-\alpha V_i(t). \tag{27}$$

Then, it can be found by (27) that

$$V_i(\tilde{t}_p)<e^{-\alpha\left(\tilde{t}_p-t_p\right)}V_i(t_p) \tag{28}$$

which indicates that $V_i(t)$ is decreased in the switching topology subinterval $[t_p,\tilde{t}_p)$. In the communication pause subinterval $[\tilde{t}_p,t_{p+1})$ $(p\in\mathbf{N})$, differentiating $V_i(t)$ along the trajectories of subsystems (14), it can be derived that

$$\dot{V}_i(t)=\hat{\boldsymbol{x}}_i^{\mathrm{T}}(t)\hat{\boldsymbol{H}}^{-1}\left(\boldsymbol{A}\hat{\boldsymbol{H}}+\hat{\boldsymbol{H}}\boldsymbol{A}^{\mathrm{T}}\right)\hat{\boldsymbol{H}}^{-1}\hat{\boldsymbol{x}}_i(t). \tag{29}$$

Let

$$\hat{\boldsymbol{M}}_2=\boldsymbol{A}\hat{\boldsymbol{H}}+\hat{\boldsymbol{H}}\boldsymbol{A}^{\mathrm{T}}-\beta\hat{\boldsymbol{H}}<0,\quad\beta>0, \tag{30}$$

then it can be shown from (22) and (29) that

$$\dot{V}_i(t)<\beta V_i(t). \tag{31}$$

Then, it immediately follows from (31) that

$$V_i(t_{p+1})<\mathrm{e}^{\beta\left(t_{p+1}-\tilde{t}_p\right)}V_i(\tilde{t}_p), \tag{32}$$

which implies that $V_i(t)$ may be increased in the communication pause subinterval $[\tilde{t}_p,t_{p+1})$. Note that $V_i(t)$ $(t\in[\tilde{t}_p,t_{p+1}))$ is decreased when the system matrix $\boldsymbol{A}<0$.

Combining (28) and (32) gives

$$V_i(t_{p+1})<\mathrm{e}^{\beta\left(t_{p+1}-\tilde{t}_p\right)-\alpha\left(\tilde{t}_p-t_p\right)}V_i(t_p). \tag{33}$$

Due to $\omega_p=(t_{p+1}-\tilde{t}_p)/(t_{p+1}-t_p)$, it can be deduced that

$$V_i(t_{p+1})<\mathrm{e}^{((\alpha+\beta)\omega_p-\alpha)(t_{p+1}-t_p)}V_i(t_p). \tag{34}$$

If $\alpha(1-\hat{\omega})>\beta\hat{\omega}\mathrm{e}^{\beta\hat{\omega}t_{\max}}$, then $\mathrm{e}^{((\alpha+\beta)\omega_p-\alpha)(t_{p+1}-t_p)}<1$ holds. Thus, according to (33), it can be found that $V_i(t)$ is exponentially decreased in the interval $[t_p,t_{p+1})$ $(p\in\mathbf{N})$. When $p=0$, it can be deduced from (34) that in the first interval $[t_0,t_1)$:

$$V_i(t_1)<\mathrm{e}^{((\alpha+\beta)\omega_0-\alpha)(t_1-t_0)}V_i(0). \tag{35}$$

Let $\kappa_p=((\alpha+\beta)\omega_p-\alpha)(t_{p+1}-t_p)$ $(p=0,1,\cdots,\tau)$, then it can be derived from (34) that

$$V_i(t_\tau)<\mathrm{e}^{\sum_{p=0}^{\tau-1}\kappa_p}V_i(0). \tag{36}$$

For any time $t_\tau<t<t_{\tau+1}$, based on the increased/decreased properties analysis from (28), (32), and (34), it follows from (36) that

$$V_i(t)<\mathrm{e}^{\sum_{p=0}^{\tau-1}\kappa_p}V_i(0). \tag{37}$$

Due to $\tau t_{\min}\leqslant t\leqslant(\tau+1)t_{\max}$, it can be derived that

$$\sum_{p=0}^{\tau-1}\kappa_p\leqslant\frac{((\alpha+\beta)\hat{\omega}-\alpha)t_{\min}}{t_{\max}}(t-t_{\max}). \tag{38}$$

Substituting (38) into (37) yields

$$V_i(t)<\mathrm{e}^{-((\alpha+\beta)\hat{\omega}-\alpha)t_{\min}}\mathrm{e}^{((\alpha+\beta)\hat{\omega}-\alpha)t_{\min}t_{\max}^{-1}t}V_i(0). \tag{39}$$

Then, it can be derived that

$$\lim_{t\to+\infty}V_i(t)=0. \tag{40}$$

Since $\hat{\boldsymbol{H}}$ is symmetric and positive definite, it can be deduced by (22) that

$$\lim_{t\to+\infty}\hat{\boldsymbol{x}}_i(t)=\boldsymbol{0},\ \ i=2,3,\cdots,N, \tag{41}$$

which means that subsystem (14) is asymptotically stable. Thus, it can be shown that leader-following DMAS (1) with control protocol (2) can achieve the desired time-varying formation with the gain matrix $\boldsymbol{K}=\lambda_{\min}^{-1}\boldsymbol{B}^{\mathrm{T}}\hat{\boldsymbol{H}}^{-1}$.

Let $\widehat{\boldsymbol{x}}(t)=[\widehat{\boldsymbol{x}}_2^{\mathrm{T}}(t),\widehat{\boldsymbol{x}}_3^{\mathrm{T}}(t),\cdots,\widehat{\boldsymbol{x}}_N^{\mathrm{T}}(t)]^{\mathrm{T}}$, then it can be deduced by control protocol (2) that

$$E=\sum_{p=0}^{+\infty}\int_{t_p}^{\tilde{t}_p}\widehat{\boldsymbol{x}}^{\mathrm{T}}(t)\left((\boldsymbol{L}_{\sigma(t)}^{\mathrm{ff}}+\boldsymbol{L}_{\sigma(t)}^{\mathrm{fl}})^2\otimes\boldsymbol{K}^{\mathrm{T}}\hat{\boldsymbol{Q}}\boldsymbol{K}\right)\widehat{\boldsymbol{x}}(t)\mathrm{d}t. \quad (42)$$

By (14) and (42), one has

$$E=\sum_{i=2}^{N}\sum_{p=0}^{+\infty}\int_{t_p}^{\tilde{t}_p}(\lambda_{\sigma(t),i})^2\hat{\boldsymbol{x}}_i^{\mathrm{T}}(t)\boldsymbol{K}^{\mathrm{T}}\hat{\boldsymbol{Q}}\boldsymbol{K}\hat{\boldsymbol{x}}_i(t)\mathrm{d}t. \quad (43)$$

Substituting $\boldsymbol{K}=\lambda_{\min}^{-1}\boldsymbol{B}^{\mathrm{T}}\hat{\boldsymbol{H}}^{-1}$ into (43) yields

$$E=\sum_{i=2}^{N}\sum_{p=0}^{+\infty}\int_{t_p}^{\tilde{t}_p}\left(\lambda_{\min}^{-1}\lambda_{\sigma(t),i}\right)^2\hat{\boldsymbol{x}}_i^{\mathrm{T}}(t)\hat{\boldsymbol{H}}^{-1}\boldsymbol{B}\hat{\boldsymbol{Q}}\boldsymbol{B}^{\mathrm{T}}\hat{\boldsymbol{H}}^{-1}\hat{\boldsymbol{x}}_i(t)\mathrm{d}t. \quad (44)$$

Due to $0=\lambda_{\sigma(t),1}<\lambda_{\min}\leqslant\lambda_{\sigma(t),i}\leqslant\lambda_{\max}$ $(i=2,3,\cdots,N)$, it immediately follows from (44) that

$$E\leqslant\sum_{i=2}^{N}\sum_{p=0}^{+\infty}\int_{t_p}^{\tilde{t}_p}\left(\lambda_{\min}^{-1}\lambda_{\max}\right)^2\hat{\boldsymbol{x}}_i^{\mathrm{T}}(t)\hat{\boldsymbol{H}}^{-1}\boldsymbol{B}\hat{\boldsymbol{Q}}\boldsymbol{B}^{\mathrm{T}}\hat{\boldsymbol{H}}^{-1}\hat{\boldsymbol{x}}_i(t)\mathrm{d}t. \quad (45)$$

Thus, it can derived by (26), (30), and (45) that

$$\begin{aligned}E\leqslant&\sum_{i=2}^{N}\sum_{p=0}^{+\infty}\int_{t_p}^{\tilde{t}_p}\hat{\boldsymbol{x}}_i^{\mathrm{T}}(t)\hat{\boldsymbol{H}}^{-1}\left(\hat{\boldsymbol{M}}_1+\left(\lambda_{\min}^{-1}\lambda_{\max}\right)^2\boldsymbol{B}\hat{\boldsymbol{Q}}\boldsymbol{B}^{\mathrm{T}}\right)\hat{\boldsymbol{H}}^{-1}\hat{\boldsymbol{x}}_i(t)\mathrm{d}t+\\&\sum_{i=2}^{N}\sum_{p=0}^{+\infty}\int_{\tilde{t}_p}^{t_{p+1}}\hat{\boldsymbol{x}}_i^{\mathrm{T}}(t)\hat{\boldsymbol{H}}^{-1}\hat{\boldsymbol{M}}_2\hat{\boldsymbol{H}}^{-1}\hat{\boldsymbol{x}}_i(t)\mathrm{d}t-\\&\sum_{i=2}^{N}\sum_{p=0}^{+\infty}\int_{t_p}^{\tilde{t}_p}\hat{\boldsymbol{x}}_i^{\mathrm{T}}(t)\hat{\boldsymbol{H}}^{-1}\left(\hat{\boldsymbol{M}}_1-\alpha\boldsymbol{H}\right)\hat{\boldsymbol{H}}^{-1}\hat{\boldsymbol{x}}_i(t)\mathrm{d}t-\\&\sum_{i=2}^{N}\sum_{p=0}^{+\infty}\int_{\tilde{t}_p}^{t_{p+1}}\hat{\boldsymbol{x}}_i^{\mathrm{T}}(t)\hat{\boldsymbol{H}}^{-1}\left(\hat{\boldsymbol{M}}_2+\beta\hat{\boldsymbol{H}}\right)\hat{\boldsymbol{H}}^{-1}\hat{\boldsymbol{x}}_i(t)\mathrm{d}t-\\&\alpha\sum_{i=2}^{N}\sum_{p=0}^{+\infty}\int_{t_p}^{\tilde{t}_p}\hat{\boldsymbol{x}}_i^{\mathrm{T}}(t)\hat{\boldsymbol{H}}^{-1}\hat{\boldsymbol{x}}_i(t)\mathrm{d}t+\beta\sum_{i=2}^{N}\sum_{p=0}^{+\infty}\int_{\tilde{t}_p}^{t_{p+1}}\hat{\boldsymbol{x}}_i^{\mathrm{T}}(t)\hat{\boldsymbol{H}}^{-1}\hat{\boldsymbol{x}}_i(t)\mathrm{d}t.\end{aligned} \quad (46)$$

From (25) and (29), one has

$$\begin{aligned}&\sum_{i=2}^{N}\sum_{p=0}^{+\infty}\int_{t_p}^{\tilde{t}_p}\hat{\boldsymbol{x}}_i^{\mathrm{T}}(t)\hat{\boldsymbol{H}}^{-1}\left(\hat{\boldsymbol{M}}_1-\alpha\hat{\boldsymbol{H}}\right)\hat{\boldsymbol{H}}^{-1}\hat{\boldsymbol{x}}_i(t)\mathrm{d}t+\\&\sum_{i=2}^{N}\sum_{p=0}^{+\infty}\int_{\tilde{t}_p}^{t_{p+1}}\hat{\boldsymbol{x}}_i^{\mathrm{T}}(t)\hat{\boldsymbol{H}}^{-1}\left(\hat{\boldsymbol{M}}_2+\beta\hat{\boldsymbol{H}}\right)\hat{\boldsymbol{H}}^{-1}\hat{\boldsymbol{x}}_i(t)\mathrm{d}t\geqslant\\&\sum_{i=2}^{N}\int_{0}^{+\infty}\dot{V}_i(t)\mathrm{d}t.\end{aligned} \quad (47)$$

By (26) and (46), if

$$\boldsymbol{A}\hat{\boldsymbol{H}}+\hat{\boldsymbol{H}}\boldsymbol{A}^{\mathrm{T}}-2\boldsymbol{B}\boldsymbol{B}^{\mathrm{T}}+\alpha\hat{\boldsymbol{H}}+\left(\lambda_{\min}^{-1}\lambda_{\max}\right)^2\boldsymbol{B}\hat{\boldsymbol{Q}}\boldsymbol{B}^{\mathrm{T}}<0 \quad (48)$$

holds, then linear matrix inequalities $\hat{\mathcal{R}}_1<0$ and $\hat{\mathcal{R}}_2<0$ as shown in Theorem 1 can be obtained according to the Schur lemma in [32]. Furthermore, on the basis of (30) and (48), according to the mean value theorem of integrals, it can be derived by (46) that

$$E<\sum_{i=2}^{N}V_i(0)+\sum_{i=2}^{N}\sum_{p=0}^{+\infty}(\beta V_i(t_{p+1})(t_{p+1}-\tilde{t}_p)-\alpha V_i(\tilde{t}_p)(\tilde{t}_p-t_p)). \quad (49)$$

Due to $\alpha(1-\hat{\omega})>\beta\hat{\omega}\mathrm{e}^{\beta\hat{\omega}t_{\max}}$, it can be obtained by (32) that

$$\sum_{i=2}^{N}\sum_{p=0}^{+\infty}(\beta V_i(t_{p+1})(t_{p+1}-\tilde{t}_p)-\alpha V_i(\tilde{t}_p)(\tilde{t}_p-t_p))<0. \quad (50)$$

Let $E_{\mathrm{ub}}=\sum_{i=2}^{N}V_i(0)=\sum_{i=2}^{N}\hat{\boldsymbol{x}}_i^{\mathrm{T}}(0)\hat{\boldsymbol{H}}^{-1}\hat{\boldsymbol{x}}_i(0)$, then it can be founded by (49) and (50) that

$$E<E_{\mathrm{ub}} \quad (51)$$

where E_{ub} is the upper bound of the energy consumption during the formation control process.

Due to

$$\left[\widehat{\boldsymbol{x}}_2^{\mathrm{T}}(t),\widehat{\boldsymbol{x}}_3^{\mathrm{T}}(t),\cdots,\widehat{\boldsymbol{x}}_N^{\mathrm{T}}(t)\right]^{\mathrm{T}}=([\boldsymbol{0},\boldsymbol{I}_{N-1}]\otimes\boldsymbol{I}_d)\widehat{\boldsymbol{x}}(t), \quad (52)$$

by (9) and (11), it can be derived that

$$\begin{aligned}E_{\mathrm{ub}}=&\sum_{i=2}^{N}\hat{\boldsymbol{x}}_i^{\mathrm{T}}(0)\hat{\boldsymbol{H}}^{-1}\hat{\boldsymbol{x}}_i(0)=\\&\bar{\boldsymbol{x}}^{\mathrm{T}}(0)\left(\boldsymbol{U}^{-\mathrm{T}}[\boldsymbol{0},\boldsymbol{I}_{N-1}]^{\mathrm{T}}[\boldsymbol{0},\boldsymbol{I}_{N-1}]\boldsymbol{U}^{-1}\otimes\hat{\boldsymbol{H}}^{-1}\right)\bar{\boldsymbol{x}}(0)\end{aligned} \quad (53)$$

and

$$\begin{aligned}&\sum_{i=2}^{N}\hat{\boldsymbol{x}}_i^{\mathrm{T}}(0)\hat{\boldsymbol{x}}_i(0)=\\&\bar{\boldsymbol{x}}^{\mathrm{T}}(0)\left(\boldsymbol{U}^{-\mathrm{T}}[\boldsymbol{0},\boldsymbol{I}_{N-1}]^{\mathrm{T}}[\boldsymbol{0},\boldsymbol{I}_{N-1}]\boldsymbol{U}^{-1}\otimes\boldsymbol{I}_d\right)\bar{\boldsymbol{x}}(0).\end{aligned} \quad (54)$$

According to the assumption of Definition 1, the initial conditions $\bar{\boldsymbol{x}}_i(0)=\boldsymbol{x}_i(0)-\boldsymbol{f}_i(0)$ $(i=2,3,\cdots,N)$ are bounded and not all agreement. Because $\boldsymbol{U}$ is non-singular, there must exist some $\hat{\boldsymbol{x}}_i(0)\neq\boldsymbol{0}$ $i\in\{2,3,\cdots,N\}$, then the following inequality holds:

$$\sum_{i=2}^{N}\hat{\boldsymbol{x}}_i^{\mathrm{T}}(0)\hat{\boldsymbol{x}}_i(0)>0. \quad (55)$$

Next, we can choose a positive scalar variable ℓ as the optimal parameter to construct the minimum-energy constraint as

$$E_{\min}=\ell\sum_{i=2}^{M}\hat{\boldsymbol{x}}_i^{\mathrm{T}}(0)\hat{\boldsymbol{x}}_i(0). \quad (56)$$

Due to

$$\boldsymbol{U}^{-\mathrm{T}}[\boldsymbol{0},\boldsymbol{I}_{N-1}]^{\mathrm{T}}[\boldsymbol{0},\boldsymbol{I}_{N-1}]\boldsymbol{U}^{-1}=\begin{bmatrix} N-1 & -\boldsymbol{1}_{N-1}^{\mathrm{T}} \\ -\boldsymbol{1}_{N-1} & \boldsymbol{I}_{N-1} \end{bmatrix}, \tag{57}$$

it can be obtained that

$$E_{\mathrm{ub}}=\bar{\boldsymbol{x}}^{\mathrm{T}}(0)\left(\begin{bmatrix} N-1 & -\boldsymbol{1}_{N-1}^{\mathrm{T}} \\ -\boldsymbol{1}_{N-1} & \boldsymbol{I}_{N-1} \end{bmatrix}\otimes\hat{\boldsymbol{H}}^{-1}\right)\bar{\boldsymbol{x}}(0), \tag{58}$$

and

$$E_{\min}=\bar{\boldsymbol{x}}^{\mathrm{T}}(0)\left(\begin{bmatrix} N-1 & -\boldsymbol{1}_{N-1}^{\mathrm{T}} \\ -\boldsymbol{1}_{N-1} & \boldsymbol{I}_{N-1} \end{bmatrix}\otimes\ell\boldsymbol{I}_d\right)\bar{\boldsymbol{x}}(0), \tag{59}$$

where $\begin{bmatrix} N-1 & -\boldsymbol{1}_{N-1}^{\mathrm{T}} \\ -\boldsymbol{1}_{N-1} & \boldsymbol{I}_{N-1} \end{bmatrix}$ is regarded as the relationship matrix of the energy consumption during the formation control process. Let $E_{\mathrm{ub}}<E_{\min}$, then the linear matrix inequality $\hat{\mathfrak{R}}_3<0$ is obtained. □

Remark 3 The Lyapunov function candidate is required to converge in the switching topology subinterval $[t_p,\tilde{t}_p)$ $(p\in\mathbf{N})$, and may diverge in the communication pause subinterval $[\tilde{t}_p,t_{p+1})$ $(p\in\mathbf{N})$. To restrict the convergent/divergent quantity of the Lyapunov function candidate, two coefficients are introduced. One is the convergence coefficient α, which can ensure the convergence rate of the Lyapunov function candidate is faster than α in the switching topology subintervals. The other is the divergence coefficient β, which undertakes that the Lyapunov function candidate diverges with a rate no more than β in the communication pause subintervals. Furthermore, with the maximum interval $t_{\max}$ and the maximum communication pause rate $\hat{\omega}$ being involved, the inequality $\alpha(1-\hat{\omega})>\beta\hat{\omega}\mathrm{e}^{\beta\hat{\omega}t_{\max}}$ $(\alpha>0,\beta>0)$ is introduced to ensure the convergent quantity of Lyapunov function candidate in the switching topology subinterval $[t_p,\tilde{t}_p)$ to be greater than the divergent quantity of the Lyapunov function candidate in the communication pause subinterval $[\tilde{t}_p,t_{p+1})$. Therefore, the globally asymptotic stability of subsystem (14) during the formation control process can be guaranteed, and the desired leader-following time-varying formation can be achieved.

Remark 4 The specific meaning of the minimum energy constraint can be regarded as the minimum energy reserve to ensure the formation achievable of the closed-loop system, which should be larger than the practical total energy consumption. In this paper, the total energy consumption $E=\sum_{i=2}^{N}\int_0^{+\infty}\boldsymbol{u}_i^{\mathrm{T}}(t)\hat{\boldsymbol{Q}}\boldsymbol{u}_i(t)\mathrm{d}t$ describes the global energy consumed by the formation control of all followers, where $\boldsymbol{u}_i^{\mathrm{T}}(t)\hat{\boldsymbol{Q}}\boldsymbol{u}_i(t)$ $(i=2,3,\cdots,N)$ is a quadratic form of the control protocol $\boldsymbol{u}_i(t)$ $(i=2,3,\cdots,N)$ with a weighted matrix $\hat{\boldsymbol{Q}}=\hat{\boldsymbol{Q}}^{\mathrm{T}}>0$. For a specific case, $\hat{\boldsymbol{Q}}$ can be diagonalized with each diagonal element denoting the specific proportion of each control channel of $\boldsymbol{u}_i(t)$. In this sense, $\boldsymbol{u}_i^{\mathrm{T}}(t)\hat{\boldsymbol{Q}}\boldsymbol{u}_i(t)$ $(i=2,3,\cdots,N)$ can be regarded as the inner product of $\boldsymbol{u}_i(t)$ $(i=2,3,\cdots,N)$ with the specific proportion of each control channel of $\boldsymbol{u}_i(t)$, which can describe the global energy consumption. By this way, we can construct the scalar expression of the energy consumption for the vector $\boldsymbol{u}_i(t)$ $(i=2,3,\cdots,N)$, which is a common method in the optimal control and can be referred in [33] for more details. Moreover, it should be pointed out that the total energy consumption is constructed without the physical unit, since $\boldsymbol{u}_i(t)$ $(i=2,3,\cdots,N)$ is dimensionless for the general leader-following DMAS. However, if the leader-following DMAS represents a physical system, then there is a physical unit. For example, the unit of the energy consumption index can be Joule for an electric-powered multiple quadrotor system.

Remark 5 In the actual situation, such as robots and unmanned aerial vehicles UAVs, there are different motion characteristics, dynamics and kinematics models, whose models containing the analysis of kinematics and dynamics can refer to [34]. Actually, the dynamics of each agent in the DMAS can be modeled as a second-order integrator with position and velocity states; i.e., $\boldsymbol{x}_i(t)=[x_{ip}(t),x_{iv}(t)]^{\mathrm{T}}\in\mathbf{R}^d=\mathbf{R}^2$ with $x_{ip}(t)$ and $x_{iv}(t)$ representing the position-like state and the velocity-like state (see [35−37]). For example, the control of the UAV is usually decomposed into the position-loop control and the attitude-loop control. Note that the control of the attitude loop is realized by the internal controller of each agent and can be designed independently. However, the formation control of a DMAS belongs to the position loop, which means that the dynamics of each agent can be modeled as the second-order integrator. In this paper, the dynamics of each agent are modeled as general high-order ones, which contain second-order integrator cases. Hence, the dynamics model of each agent and the corresponding method in this paper can be used in the formation research for some practical multi-agent systems, such as robots and UAVs.

Based on the aforementioned proofs, if the gain matrix $\boldsymbol{K}$ is given in advance, then sufficient conditions for minimum-energy leader-following formation achievement in the sense of linear matrix inequality is proposed below.

Theorem 2 For the given gain matrix $\boldsymbol{K}$, DMAS (1) with control protocol (2) is minimum-energy leader-following formation achievable if $\dot{\boldsymbol{f}}_i(t)=\boldsymbol{A}\boldsymbol{f}_i(t)$ $(i=2,3,\cdots,N)$, $\alpha(1-\hat{\omega})>\beta\hat{\omega}\mathrm{e}^{\beta\hat{\omega}t_{\max}}$ with $\alpha>0$ and $\beta>0$, then there exists $\hat{\boldsymbol{H}}_c^{\mathrm{T}}=\hat{\boldsymbol{H}}_c>0$ such that the following minimization problem has a minimum-energy optimal parameter ℓ_c:

$$\min \ell_c$$

$$\text{s.t.}\begin{cases}\hat{\mathfrak{R}}_{c1}=\hat{\boldsymbol{H}}_c\boldsymbol{A}+\boldsymbol{A}^{\mathrm{T}}\hat{\boldsymbol{H}}_c-\beta\hat{\boldsymbol{H}}_c<0\\ \hat{\mathfrak{R}}_{c2}=\begin{bmatrix}\boldsymbol{\wp}_c & \lambda_{\max}\boldsymbol{K}^{\mathrm{T}}\hat{\boldsymbol{Q}}\\ * & -\hat{\boldsymbol{Q}}\end{bmatrix}<0\\ \hat{\mathfrak{R}}_{c3}=\hat{\boldsymbol{H}}_c-\ell_c\boldsymbol{I}_d<0\end{cases}$$

where $\boldsymbol{\wp}_c=\hat{\boldsymbol{H}}_c\boldsymbol{A}+\boldsymbol{A}^{\mathrm{T}}\hat{\boldsymbol{H}}_c-\lambda_{\max}\boldsymbol{K}^{\mathrm{T}}\boldsymbol{B}^{\mathrm{T}}\hat{\boldsymbol{H}}_c-\lambda_{\max}\hat{\boldsymbol{H}}_c\boldsymbol{B}\boldsymbol{K}+\alpha\hat{\boldsymbol{H}}_c$. In this case, the minimum-energy constraint $E_{\min}=\bar{\boldsymbol{x}}^{\mathrm{T}}(0)\left(\begin{bmatrix}N-1 & -\boldsymbol{1}_{N-1}^{\mathrm{T}}\\ -\boldsymbol{1}_{N-1} & \boldsymbol{I}_{N-1}\end{bmatrix}\otimes\ell_c\boldsymbol{I}_d\right)\bar{\boldsymbol{x}}(0)$.

4. Numerical simulations

In this section, a numerical simulation is provided to verify the above theoretical results. Consider a DMAS with agent 1 being the leader and agents i $(i=2,3,\cdots,7)$ followers. The system matrices are

$$\begin{cases}\boldsymbol{A}=\begin{bmatrix}0 & 0 & -1\\ -6.3 & -6.3 & 1\\ -1.5 & -2.5 & 0\end{bmatrix}\\ \boldsymbol{B}=\begin{bmatrix}0 & 1\\ 1 & 0\\ 0 & 1\end{bmatrix}\end{cases}.$$

The initial states of agent i (i=1,2,$\cdots$,7) are given as $\boldsymbol{x}_1=[12,14,-25]^{\mathrm{T}}$, $\boldsymbol{x}_2=[45,28,-17]^{\mathrm{T}}$, $\boldsymbol{x}_3=[2,-81,-22]^{\mathrm{T}}$, $\boldsymbol{x}_4=[16,60,-50]^{\mathrm{T}}$, $\boldsymbol{x}_5=[-35,20,65]^{\mathrm{T}}$, $\boldsymbol{x}_6=[-15,-3,21]^{\mathrm{T}}$, $\boldsymbol{x}_7=[-15,4,-36]^{\mathrm{T}}$.

The desired leader-following formation functions are set as follows:

$$\boldsymbol{f}_1(t)=\begin{bmatrix}0 & 0 & 0\end{bmatrix}^{\mathrm{T}},$$

$$\boldsymbol{f}_i(t)=\begin{bmatrix}20\sin\left(t+\dfrac{i\pi}{3}\right)\\ -20\sin\left(t+\dfrac{i\pi}{3}\right)\\ -20\cos\left(t+\dfrac{i\pi}{3}\right)\end{bmatrix},$$

where $i=2,3,\cdots,7$.

The switching set with four topologies is presented in Fig.1, where the yellow five-pointed star represents the leader and other different color squares denote six different followers. The switch signal of randomly switching topologies and aperiodic communication pauses is shown in Fig. 2, where the time period is set as $t=10$ s and is divided by time intervals with 1.9 s, 2.2 s, 1.7 s, 2.3 s, and 1.9 s. In this case, the duration of each switching topology or each communication pause may be different, which means that the topologies are switched randomly and communication pauses are aperiodic with the maximum interval $t_{\max}=2.3$ s and the maximum communication pause rate $\hat{\omega}=0.35$.

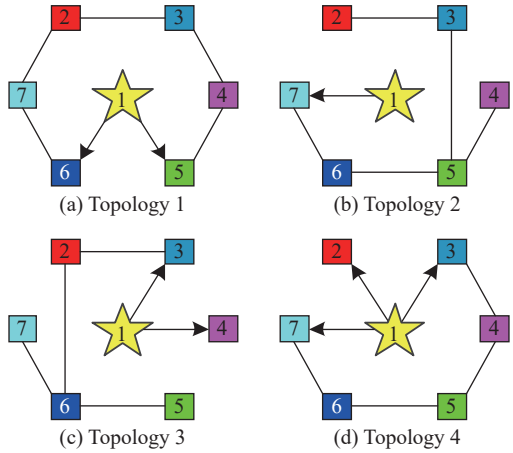

Fig. 1 Switching set

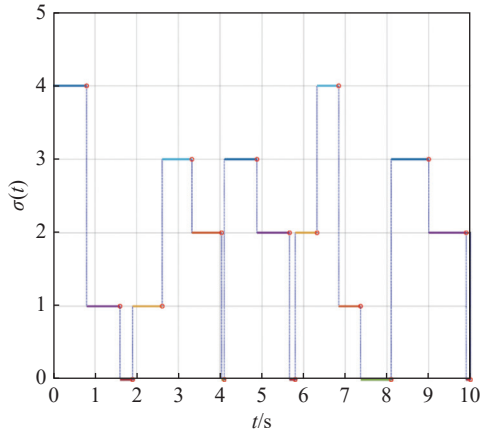

Fig. 2 Switching signal

The convergence coefficient α, the divergence coefficient β, and the weighted matrix $\hat{\boldsymbol{Q}}$ are set as $\alpha=0.8$, $\beta=0.7$, and $\hat{\boldsymbol{Q}}=\mathrm{diag}\{0.000\,5,0.000\,5\}$. It can be found that $(\boldsymbol{A},\boldsymbol{B})$ is stabilizable, and the formation feasible conditions $\dot{\boldsymbol{f}}_i(t)=\boldsymbol{A}\boldsymbol{f}_i(t)$ and the specific inequality $\alpha(1-\hat{\omega})>\beta\hat{\omega}\mathrm{e}^{\beta\hat{\omega}t_{\max}}$ are satisfied, where $i=1,2,\cdots,7$. The real symmetric matrix $\hat{\boldsymbol{H}}^{-1}$ of the Lyapunov function candidate and the minimum-energy optimal parameter ℓ are solved as

$$\hat{\boldsymbol{H}}^{-1}=\begin{bmatrix}1.582\,1 & 0.331\,4 & -1.054\,7\\ 0.331\,4 & 0.390\,0 & -0.998\,2\\ -1.054\,7 & -0.998\,2 & 2.587\,9\end{bmatrix},$$

$$\ell=3.6194,$$

respectively. Then, the gain matrix $\boldsymbol{K}$ is

$$\boldsymbol{K}=\lambda_2^{-1}\boldsymbol{B}^{\mathrm{T}}\hat{\boldsymbol{H}}^{-1}=\begin{bmatrix}3.775\,9 & 4.443\,3 & -11.373\,2\\ 6.008\,7 & -7.597\,3 & 17.468\,0\end{bmatrix}.$$

Thus, the total energy consumption with the minimum-energy constraint during the time period $t=10$ s is $E(t)|_{t=10}=331.310\,9$.

If the inequality $\hat{\mathfrak{R}}_3 = \boldsymbol{I}_d - \ell\hat{\boldsymbol{H}} < 0$ is not considered, then the conclusion of Theorem 1 will degenerate into other formation criteria as discussed in [20] and [24]. In the case, without the minimum-energy constraint, the matrix variable, the gain matrix, and the total energy consumption are represented by $\hat{\boldsymbol{H}}_F^{-1}$, $\hat{\boldsymbol{K}}_F$, and E_F respectively, which can be expressed as

$$\hat{\boldsymbol{H}}_F^{-1} = \begin{bmatrix} 2.623\ 8 & 0.523\ 7 & -1.685\ 6 \\ 0.523\ 7 & 0.629\ 7 & -1.609\ 5 \\ -1.685\ 6 & -1.609\ 5 & 4.170\ 1 \end{bmatrix},$$

$$\hat{\boldsymbol{K}}_F = \lambda_2^{-1}\boldsymbol{B}^{\mathrm{T}}\hat{\boldsymbol{H}}_F^{-1} = \begin{bmatrix} 5.966\ 4 & 7.174\ 5 & -18.337\ 6 \\ -10.688\ 8 & -12.371\ 2 & 28.306\ 9 \end{bmatrix},$$

$$E_F(t)|_{t=10} = 520.193\ 8.$$

It can be found that the total energy consumption with the minimum-energy constraint is less than the total energy consumption without the minimum-energy constraint in $t = 10$ s; i.e., $E(t)|_{t=10} < E_F(t)|_{t=10}$.

The tracking error trajectories $\boldsymbol{x}_i(t) - \boldsymbol{f}_i(t)(i = 1, 2, \cdots, 7)$ in three different dimensions with the control gain matrix $\boldsymbol{K}$ are described in Fig. 3, where the black curve with little circles depicts the trajectory of the leader. By Fig. 3, it can be found that there are some little abrupt waves in the curve, which reflect switching actions from topologies to communication pauses, or switching actions among different topologies. It can be found that the desired formation can be achieved for the case that the topologies are switched randomly and communication pauses are aperiodic. Fig. 4 exhibits position changes of the leader and six followers at the moment $t = 0$ s, 1.5 s, 3.5 s, and 4 s, where the leader and six followers are marked by a yellow five-pointed star and six squares with different colors, respectively.

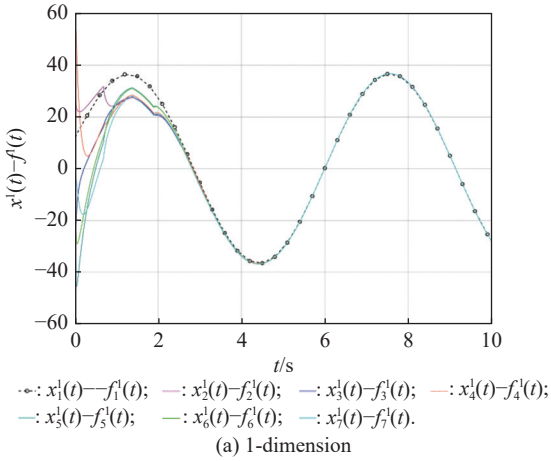

(a) 1-dimension

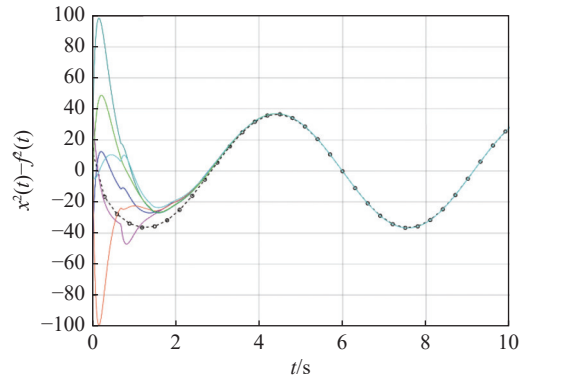

(b) 2-dimension

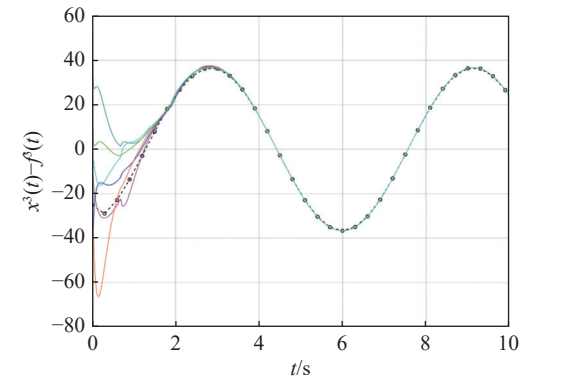

(c) 3-dimension

Fig. 3 Trajectories of $\boldsymbol{x}_i(t) - \boldsymbol{f}_i(t)$

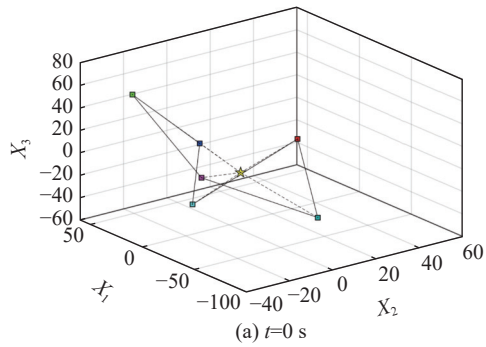

(a) t=0 s

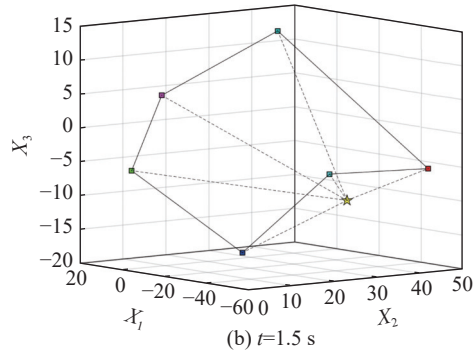

(b) t=1.5 s

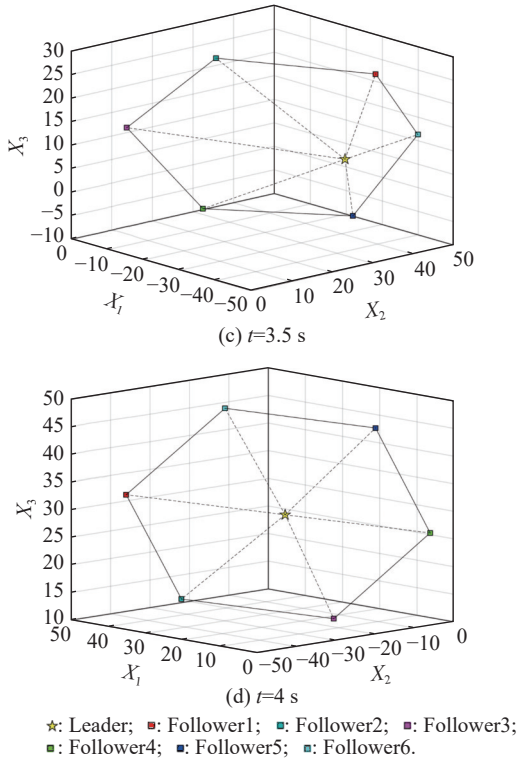

Fig. 4 Position changes of the leader and six followers

As shown in Fig. 5, the leader rotates counterclockwise within 10 s, whose trajectory is shown by the red triangle dot line and is determined by the dynamics of the leader; that is, $\dot{\boldsymbol{x}}_1(t)=\boldsymbol{A}\boldsymbol{x}_1(t)$.

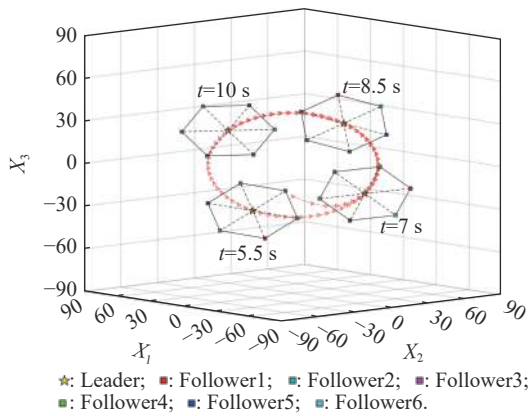

Fig. 5 Trajectory of the leader

The curves of $E(t)$ and $E_F(t)$ are shown in Fig. 6, where the two total energy consumptions trend to two different limited values. It can be found from Fig. 6 that the total energy consumption with the minimum-energy constraint is less than the one with other methods during the leader-following formation process; i.e., $E(t)<E_F(t)$. Combined with the trending curves of the tracking trajectories, position changes, and the trajectory of the leader from Fig. 3 to Fig. 5, it can be seen that six followers gradually form and continuously maintain a time-varying regular hexagon with circling the leader in the middle at the same angular velocity.

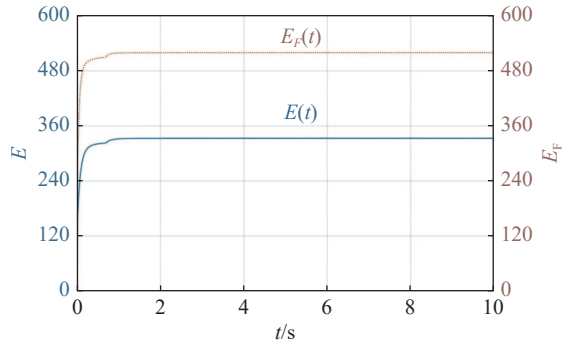

Fig. 6 Energy consumption curves $E(t)$ and $E_F(t)$

In addition, to show the difference of the simulation results with different values of parameters, the values of matrices $\boldsymbol{A}$, $\boldsymbol{B}$, the conversion coefficient α and the diffusion coefficient β are chosen as follows:

$$\boldsymbol{A}=\begin{bmatrix}1&1&-1\\-5&-5&1\\-1&-2&0\end{bmatrix},\ \boldsymbol{B}=\begin{bmatrix}0&2\\1.5&0\\0&1.5\end{bmatrix},$$

$$\alpha=0.8,\ \beta=0.5,$$

it can be found that $(\boldsymbol{A},\boldsymbol{B})$ is stabilizable, and $\dot{\boldsymbol{f}}_i(t)=\boldsymbol{A}\boldsymbol{f}_i(t)$ and $\alpha(1-\hat{\omega})>\beta\hat{\omega}\mathrm{e}^{\beta\hat{\omega}t_{\max}}$ are satisfied. With the other parameters being the same, the real symmetric matrix $\hat{\boldsymbol{H}}^{-1}$ of the Lyapunov function candidate and the minimum-energy optimal parameter ℓ are solved as

$$\hat{\boldsymbol{H}}^{-1}=\begin{bmatrix}0.463\,0&0.123\,6&-0.158\,0\\-0.158\,0&-0.244\,0&0.479\,9\\0.123\,6&0.128\,6&-0.244\,0\end{bmatrix},$$

$$\ell=0.767\,0,$$

respectively. Then, the gain matrix $\boldsymbol{K}$ is

$$\boldsymbol{K}=\lambda_2^{-1}\boldsymbol{B}^{\mathrm{T}}\hat{\boldsymbol{H}}^{-1}=\begin{bmatrix}2.111\,9&2.197\,3&-4.169\,3\\7.849\,8&-1.353\,4&4.601\,4\end{bmatrix}.$$

In this case, the total energy consumption with the minimum-energy constraint during the time period is $E(t)|_{t=10}=75.311\,2$. From the above simulation results, it can be found that the different values of $\boldsymbol{A}$, $\boldsymbol{B}$, α, and β may lead to the different gain matrix design, but the minimum-energy formation can be achieved by the associated gain matrix. Thus, it can be found that DMAS (1) with control protocol (2) can achieve the desired leader-following time-varying formation with the minimum-energy constraint in the sense of the linear matrix inequality under the communication constraints of randomly switching topologies and aperiodic communication pauses.

5. Conclusions

Minimum-energy time-varying formation problems of the leader-following DMAS subjected to randomly switching topologies and aperiodic communication pauses are addressed in this paper. Based on the proposed formation control protocol with the total energy consumption being involved, criteria of design and analysis for the minimum-energy formation are proposed, which can be checked by the generalized eigenvalue method. Especially, variables in criteria that are required to be solved are independent on the number of agents, which can guarantee the scalability of the DMAS. By a two-step transformation approach, the asymmetric Laplacian matrix of the leader-following DMAS topology is well dealt with. Furthermore, the minimum-energy constraint can be determined, which is associated with the initial conditions and the relationship matrix, where the relationship matrix is the Laplacian matrix of the star graph with the interaction weight being one. In the further work, the minimum-energy leader-following formation control problems with jointly spanning tree topologies will be further researched.

References

[1] PARTOVIBAKHSH M, LIU G J. An adaptive unscented Kalman filtering approach for online estimation of model parameters and state-of-charge of lithium-ion batteries for autonomous mobile robots. IEEE Trans. on Automatic Control, 2014, 23(1): 357–363.

[2] KIM C J, CHWA D. Obstacle avoidance method for wheeled mobile robots using interval type-2 fuzzy neural network. IEEE Trans. on Fuzzy System, 2015, 23(3): 677–687.

[3] ZHANG D, CAI W J, XIE L H, et al. Nonfragile distributed filtering for T-S fuzzy systems in sensor networks. IEEE Trans. on Fuzzy System, 2015, 23(5): 1883–1890.

[4] CHEN S, HO D W C, HUANG C. Fault reconstruction and state estimator design for distributed sensor networks in multi target tracking. IEEE Trans. on Industrial Electronics, 2015, 62(11): 7091–7102.

[5] DONG X W, YU B C, SHI Z Y, et al. Time-varying formation control for unmanned aerial vehicles: theories and applications. IEEE Trans. on Control Systems Technology, 2015, 23(1): 340–348.

[6] QI Y H, ZHOU S L, KANG Y H, et al. Formation control for unmanned aerial vehicles with directed and switching topologies. International Journal of Aerospace Engineering, 2016, 2016: 7657452.

[7] DANG Z H, ZHANG Y L. Control design and analysis of an inner-formation flying system. IEEE Trans. on Aerospace and Electronic Systems, 2015, 51(3): 1621–1634.

[8] HUANG X L, ZHANG C, LU H Q, et al. Adaptive reaching law based sliding mode control for electromagnetic formation flight with input saturation. Journal of the Franklin Institute, 2016, 353(11): 2398–2417.

[9] WANG L, XI J X, HOU B, et al. Limited-budget consensus design and analysis for multiagent systems with switching topologies and intermittent communications. IEEE/CAA Journal of Automatica Sinica, 2021, 8(10): 1724–1736.

[10] ABBSL Y, MOOSAVIAN S A A, NOVINZADEH A B. Formation control of aerial robots using virtual structure and new fuzzy based self-tuning synchronization. Transactions of the Institute Measurement and Control, 2017, 39(12): 1906–1919.

[11] BALCH T, ARKIN R C. Behavior-based formation control for multirobot teams. IEEE Trans. on Robot Automatic, 1998, 14(6): 926–939.

[12] LIN J L, HWANG K S, WANG Y L, et al. A simple scheme for formation control based on weighted behavior learning. IEEE Trans. on Neural Networks and Learning Systems, 2013, 25(6): 1033–1044.

[13] LORIA A, DASDEMIR J, JARQUIN N A. Leader-follower formation and tracking control of mobile robots along straight paths. IEEE Trans. on Control Systems Technology, 2015, 24(2): 727–732.

[14] YANG X J, LIAO L J, YANG Q, et al. Limited-energy output formation for multiagent systems with intermittent interactions. Journal of the Franklin Institute, 2021, 358(13): 6462–6489.

[15] LI J L, XI J X, HE M, et al. Formation control for networked multiagent systems with a minimum energy constraint. Chinese Journal of Aeronautics, 2023, 36(1): 342–355.

[16] REN W. Consensus strategies for cooperative control of vehicle formations. IET Control Theory Application, 2007, 1(2): 505–512.

[17] ANDERSSON M, WALLANDER J. Kin selection and reciprocity in flight formation. Behavioral Ecology, 2004, 15(1): 158–162.

[18] REN W, SORENSEN N. Distributed coordination architecture for multirobot formation control. Robotics and Autonomous Systems, 2008, 56(4): 324–333.

[19] BRINON-ARRANZ L, SEURET A, CANUDAS-DE-WIT C. Cooperative control design for time-varying formations of multi-agent systems. IEEE Trans. on Automatic Control, 2014, 59(8): 2283–2288.

[20] YOO S J, KIM T H. Distributed formation tracking of networked mobile robots under unknown slippage effects. Automatica, 2015, 54: 100–106.

[21] YAN C H, ZHANG W, LI X H, et al. Observer-based time-varying formation tracking for one-sided Lipschitz nonlinear systems via adaptive protocol. International Journal of Control Automation and Systems, 2020, 18(12): 2753–2764.

[22] LIU X F, XIE Y F, LI F B, et al. Formation control of singular multiagent systems with switching topologies. International Journal of Robust Nonlinear Control, 2020, 30(2): 652–664.

[23] XI J X, WANG L, ZHENG J F, et al. Energy-constraint formation for multiagent systems with switching interaction topologies. IEEE Trans. on Circuits and Systems-I: Regular papers, 2020, 67(7): 2442–2454.

[24] YANG X, HUA C C, YAN J, et al. Adaptive formation control of cooperative teleoperators with intermittent communications. IEEE Trans. on Cybernetics, 2018, 49(7): 2514–2523.

[25] CHAI X F, LIU J, YU Y, et al. Practical fixed-time event-triggered time-varying formation tracking control for dis-

turbed multi-agent systems with continuous communication free. Unmanned Systems, 2021, 9(1): 1–12.
[26] CAO Y C, REN W. Optimal linear-consensus algorithms: an LQR perspective. IEEE Trans. on Systems, Man, and Cybernetics-Part B:Cybernetics, 2010, 40(3): 819–829.
[27] ZHAO Y D, ZHANG W D. Guaranteed cost consensus protocol design for linear multi-agent systems with sampled-data information: an input delay approach. ISA Transactions, 2017, 67: 87–97.
[28] WANG Z, HE M, ZHENG T, et al. Guaranteed cost consensus for high-dimensional multi-agent systems with time-varying delays. IEEE/CAA Journal of Automatica Sinica, 2018, 5(1): 181–189.
[29] YU J L, DONG X W, LI Q D, et al. Robust guaranteed cost time-varying formation tracking for high-order multiagent systems with time-varying delays. IEEE Trans. on Systems Man Cybernetics: Systems, 2020, 50(4): 1465–1475.
[30] XI J X, WANG C, YANG X J, et al. Limited-budget output consensus for descriptor multiagent systems with energy constraints. IEEE Trans. on Cybernetics, 2020, 50(11): 4585–4598.
[31] GODSIL C, ROYLE G. Algebraic graph theory. New York: Springer-Verlag, 2001.
[32] YU W W, CAO J D, WANG J. An LMI approach to global asymptotic stability of the delayed Cohen-Grossberg neural network via nonsmooth analysis. Neural Networks, 2007, 20(7): 810–818.
[33] ANDERSON B D O, MOORE J B. Optimal control: linear quadratic methods. New York: Dover publications, 2007.
[34] LIN Z Y, DING W, YAN G F, et al. Leader-follower formation via complex Laplacian. Automatica, 2013, 49(6): 1900−1906.
[35] DONG X W, ZHOU Y, REN Z, et al. Time-varying formation tracking for second-order multi-agent systems subjected to switching topologies with application to quadrotor formation flying. IEEE Trans. on Industrial Electronics, 2017, 64(6): 5014–5024.
[36] WANG J N, XIN M. Integrated optimal formation control of multiple unmanned aerial vehicles. IEEE Trans. on Control Systems Technology, 2013, 21(5): 1731−1744.
[37] WANG J N, BI C Y, WANG D D, et al. Finite-time distributed event-triggered formation control for quadrotor UAVs with experimentation. ISA Transactions, 2022, 126: 585−596.

Biographies

QIN Donghao was born in 1978. He received his B.S. degree from Taiyuan University of Science and Technology, Taiyuan, China, and M.S. degree from Northwestern Polytechnical University, Xi'an, China, in 2000 and 2010, respectively. He is currently pursuing his Ph.D. degree in control science and engineering from Rocket Force University of Engineering, Xi'an, China. His research interests include multi-agent systems, optimal control, and formation control.
E-mail: 42606553@qq.com

WANG Le was born in 1991. He received his B.S., M.S. and Ph.D. degrees from Rocket Force University of Engineering, Xi'an, China in 2014, 2016, and 2020, respectively. He is currently a lecturer in control science and engineering of Rocket Force University of Engineering, China. His research interests include optimal control, fault tolerant control, and multiagent systems.
E-mail: wangaz14@163.com

GAO Jiuan was born in 1990. He received his B. S. and M. S. degrees in Northwestern Polytechnical University, Xi'an, China in 2011 and 2014, respectively. He is now a lecturer in control science and engineering of Rocket Force University of Engineering. His research interests include swarm systems, and control and navigation for flight vehicle.
E-mail: gaojiuan6@126.com

XI Jianxiang was born in 1981. He received his B.S. and M.S. degrees from Rocket Force University of Engineering, Xi'an, China in 2004 and 2007, respectively. He received his Ph.D. degree in control science and engineering from Rocket Force University of Engineering, Xi'an, China in 2012 by a coalition form with Tsinghua University. He is currently a professor in control science and engineering of Rocket Force University of Engineering, China. His research interests include complex systems control, switched systems and swarm systems.
E-mail: xijx07@mails.tsinghua.edu.cn